Optik 114, No. 4 (2003) 161–167

http://www.urbanfischer.de/journals/optik

Optik Optics
International Journal for Light and Electron Optics

Compact, reliable asymmetric optical configuration for cost-effective fabrication of multiplex dot matrix hologram in anti-counterfeiting applications

Ying Tsung Lu[1, 2], Sien Chi[1]

[1] Institute of Electro-Optical Engineering, National Chiao-Tung University, 1001 Ta Hsueh Rd., Hsinchu, Taiwan, R.O.C
[2] Opto-Electronics & Systems Laboratories, Industrial Technology Research Institute, Bldg. 51, 195-8 Sec. 4, Chung Hsing Rd., Chutung, Taiwan 310, R.O.C.

Abstract: This study presents a compact optical configuration that can generate a multiplex dot-matrix hologram with complex interlaced images for anti-counterfeiting applications on valuable paper. Varying the orientation of the interference plane can enable the multiplex hologram to be recorded without changing the interference angle of two laser beams. With its simple asymmetric optical setup, a multiplex hologram with many interlaced images can be efficiently fabricated, increasing the cost of imitation. Experimental details of the asymmetric optical setup are also described.

Key words: Multiplex images – dot-matrix hologram – security hologram – anti-counterfeiting

1. Introduction

Holograms have long been employed in anti-counterfeiting. Their unique light characteristics make them useful in the securing valuable papers. Examples include banknote in Singapore, Californian driving license, Germany and Taiwanese passports, credit cards, and even entrance tickets to Super Bowl Game of the National Football League. In the past, most authentication holograms have been of the rainbow type [1]. However, the manufacturing cost has always been high because of the difficult work of sculpting a model and the need for expensive manufacturing optical facilities. Much research has focused on developing advanced hologram technologies that can display 2-D or 3-D images without traditional holography [2–9]. A dot-matrix hologram integrated with small grating dots obtained by the interference of two laser beams is one practical technology. Such a hologram can be complex with single or multiplex images, created with the assistance of a computer. Much of the literature reported the progress of dot-matrix hologram technologies [9–14]. However, most optical systems are designed for symmetric interference. The disadvantage is that such systems are always bulky and involve complicated optical components, driving electronics and moving devices that are difficult to operate and maintain. The fabrication of a hologram is thus not cost-effective.

This work presents a compact, asymmetric setup of a hologram printer [15] to generate cost-effectively a multiplex dot-matrix hologram for anti-counterfeiting applications.

Received 6 January 2003; accepted 25 March 2003.

Correspondence to: Y. T. Lu
Fax: ++886-3-5917479
E-mail: lit@itri.org.tw

2. Theoretical background

Basic concept of dot-matrix hologram

A picture can be "pixelized" as a matrix of bit elements. Replacing the bit elements of a picture with grating dots of the same size and all with the same grating vector, enables the images to be diffracted in a specific direction under uniform illumination of white light: the images are not viewable in any direction. Images can thus be projected in specified directions by constructing individual interlaced images with grating dots of different orientations (grating vectors). Interlaced images can be either generated by computer or imported from an image scanner. Any such images can thus be devised. The process can present obstacles to counterfeiting.

The reconstructed beam incident on a grating is assumed to be [16]

$$U_i(\boldsymbol{r}) = A_i(\boldsymbol{r}) \exp\left(-\mathrm{i}\boldsymbol{k}_\mathrm{i} \cdot \boldsymbol{r}\right). \quad (1)$$

The incident wave is taken to be a plane wave because a hologram is always observed at an appropriate distance from a light source. Analogously, the complex amplitude of the wave diffracted from the hologram will be

$$U_d(\boldsymbol{r}) = A_d(\boldsymbol{r}) \exp\left(-\mathrm{i}\boldsymbol{k}_d \cdot \boldsymbol{r}\right), \quad (2)$$

0030-4026/03/114/04-161 $ 15.00/0

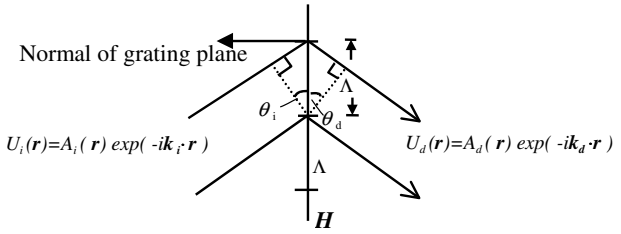

Fig. 1. The beams diffracted from a thin grating.

where $A_i(\boldsymbol{r})$ and $A_d(\boldsymbol{r})$ are the amplitudes of the incident and diffractive waves, respectively, at an arbitrary coordinate, $r \cdot \boldsymbol{k}_i$ and $\boldsymbol{k}_d$ are the wave vectors of the incident and diffractive wave, respectively. A surface relief grating is like a "planar" grating because the grating is formed only on the surface of a hologram. The discussion can thus be confined to diffraction in the Raman-Nath regime, rather than Bragg diffraction [17]. Only the first diffraction order is considered because it dominates the diffraction from a grating. Therefore, for a grating, *H,* depicted in fig. 1, the diffraction relationship between the incident beam and the first order diffraction beam can be written as [18]

$$\frac{\sin\theta_d}{\lambda} = \frac{\sin\theta_i}{\lambda} - \frac{1}{\Lambda}, \tag{3}$$

where λ is the wavelength of an incident beam , and Λ is the period of the grating. The equation can also be expressed as [19]

$$\boldsymbol{k}_d = \boldsymbol{k}_i - \boldsymbol{K}, \tag{4}$$

where $|\boldsymbol{K}| = 2\pi/\Lambda$ is the grating vector. Figure 1 shows the vectors and their relationship. θ_d and θ_i are the angles of intersection of the incident and diffraction beam with the normal of the grating surface, respectively. Λ is the period of the grating. Equation (4) shows that the diffraction wave vector, $\boldsymbol{k}_d$, is determined from the grating vector, $\boldsymbol{K}$, under an incident beam, $\boldsymbol{k}_i$, with a fixed illumination direction.

In general, a hologram with a surface relief grating can be distinguished as either a transmission or reflection type. In commercial applications, a reflection type hologram is more practical than a transmission type

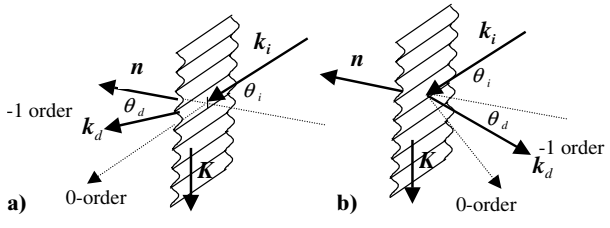

Fig. 2. The geometric relation of diffraction of wave vectors in transmission and reflection grating. a) The diffraction relation of wave vectors of a transmission type grating with sinusoidal relief surface. b) The diffraction relation of wave vectors of a grating with aluminum coating on the surface.

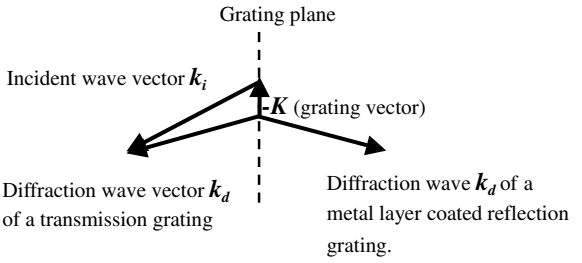

Fig. 3. The diffraction wave vector from a transmission grating (left side) and a reflection grating (right side).

hologram. Figure 2 shows the diffraction behavior of a transmission hologram and a reflection hologram, respectively. Figure 2b shows that the diffraction beam bounces back to the same side as the incident beam when the transmission hologram (a) is coated with an Aluminum layer to form a reflection hologram. The diffraction direction, $\boldsymbol{k}_d$, in (b) is a mirror mapping of the one in (a). Figure 3 schematically depicts the relationship between the diffraction vectors of transmission and reflection holograms. According to eq. (4), and figs. 1, 2, and 3, $\boldsymbol{k}_d$ varies with $\boldsymbol{K}$ for fixed $\boldsymbol{k}_i$. Figure 4 shows the effect. The separation of the diffraction beams (i.e. the difference of $\boldsymbol{k}_d$) from different gratings depends on the difference between their $\boldsymbol{K}$ orientations. Consequently, the separation of images increases with the difference between the orientation of the gratings.

Multiplex images

Images mixed in the hologram are synthesized by computer before fabrication. Each pixel of the images is transferred as a grating dot in a position that corresponds to the position on the hologram. A multiplex hologram with four images, *"A", "B", "C", "D",* was used as an example for describing the concept. Fig. 5a shows the hologram divided into matrix elements. Each element can include up to four grating dots with different $\boldsymbol{K}$ values. Fig. 5b shows the directions of dif-

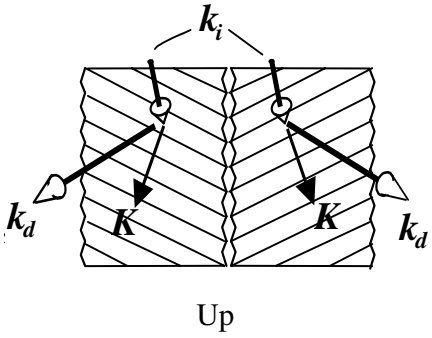

Fig. 4. The wave vectors diffracted from grating with various orientations under identical illumination.

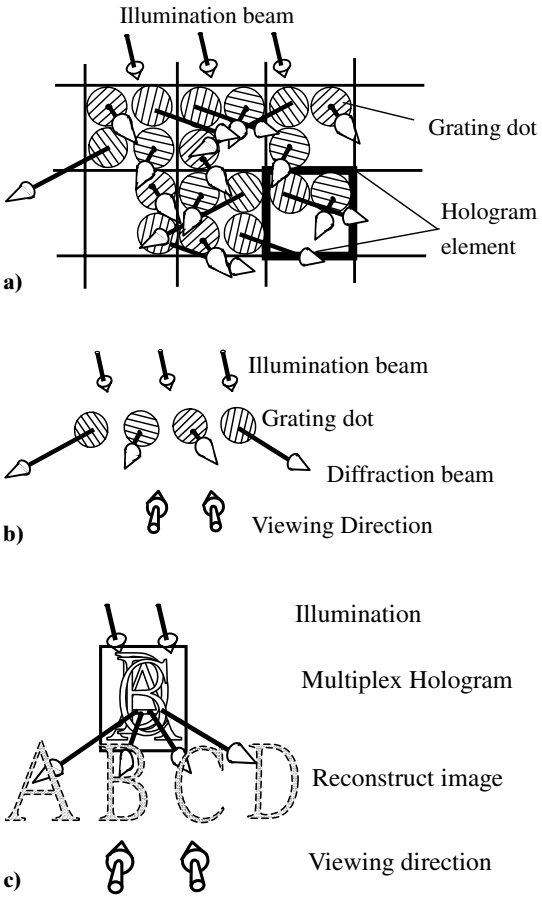

Fig. 5. a) The rectangular areas blocked by black thick line show the hologram elements, each element includes four dots. Each dot construct a pixel of each image. b) The dots with different grating vector and their corresponding diffraction direction in different viewing position. c) The images diffracted from hologram one by one when moving the eyes across the hologram under a fixed illumination.

fraction from gratings with various orientations. The multiplex images will be observed consecutively, when a viewer's eyes move across the hologram, as shown in fig. 5c, because each image is constructed of dots with the same orientation from each element in the hologram. The same phenomenon will be observed by wavering the hologram under illumination by white light.

3. Setup and experiment

Figure 6 depicts the setup of the dot-matrix hologram printer. The laser beam passes through a focusing lens, designed to adjust the size of the beam spot on the recording plane, by moving the lens along the rail. A shutter set to switch the laser beam on/off for each exposure. The photoresist plate is put on a holder on the XY stage to record the image for recording. The rotary disc utilized to change the orientation of the interfer-

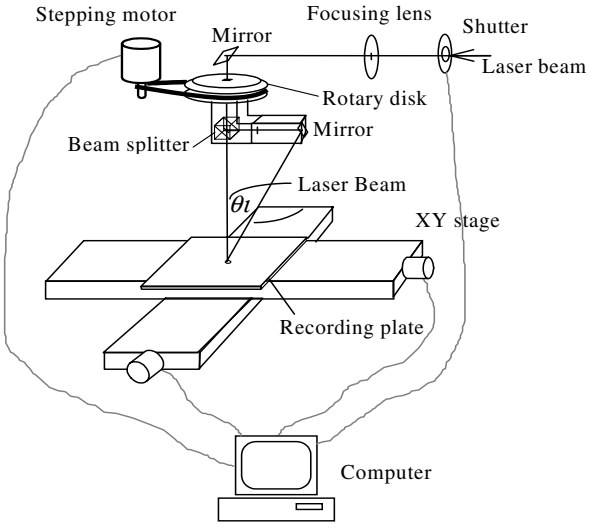

Fig. 6. Diagram of dot-matrix hologram fabrication system with asymmetric optical setup.

ence is a critical part of the setup. A combination of a cube beam splitter and a mirror is fixed under the rotary disc. The beam splitter splits the laser beam into two parts with equal intensity. One is reflected from the mirror and the other passes through the beam splitter directly to the recording plane. They intersect on the recording plane at the proper angle. When the rotary disc is rotated, the orientation of the reflection beam changes but the beam continues to overlap with the transmitted beam on the recording plate, changing the orientation of the interference and thus varying the grating vector. The paths of the two beams are designed to be unequal with non-symmetric intersect angles with the normal to the hologram. The design is based on improving rigidity and stability for operation. In this experiment, the performance of the hologram does not differ significantly between the asymmetric and the symmetric arrangement. The asymmetric compact setup can operate at a very high speed, over a long period of operation and tens of exposures per second.

The intersection angle between the two laser beams is determined from the condition of hologram reconstruction under common illumination. According to eq. (4), and the previous section, the grating vector, $\boldsymbol{K}$, which is determined by the interference angle between the two beams, dominates the direction of diffraction. Figure 7 schematically depicts reconstruction of a hologram. White light illuminates the hologram at an incident angle of θ from the normal. The diffraction direction is set to coincide with the normal of hologram plane. Therefore

$$K = k_i \sin\theta\,, \tag{5}$$

where θ is the angle between the illumination beam and diffraction beam [20]. Clearly the angle of intersec-

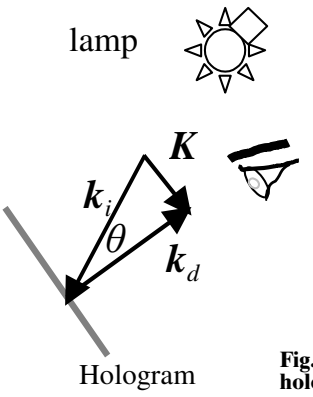

Fig. 7. The reconstruction of a hologram.

tion, θ_i of the two interference laser beams equals θ. In general, the common illumination angle (θ) is between 20 and 30 degrees from the normal. Thus θ_i is also within 20 and 30 degrees from the hologram normal.

Theoretically, the total orientation range of the grating direction could be cover almost 180 degrees (180 degrees exactly is eliminated because it represents the same diffraction condition as 0 degree) without diffracting two images in the same direction. In case of a multiplex with four images, the theoretical angular separation of the gratings should be 180 degrees/3 = 60 degrees, to split the images properly and to prevent overlapping with an adjacent image. Empirically, a total orientation range of 90 degrees can separate the images sufficiently.

The exposure time of each dot depends on the intensity of exposure. For a He-Cd (@442 nm) laser with an output power of tens of mW, the exposure time per dot could be less than 100 milliseconds. The size of the dot on the hologram is determined from the size of the input beam and the focal length of the focusing lens. The focusing lens can be adjusted along the rail to control the spot size, as shown in fig. 8a. The grating dots with about 1000 dpi (dot diameter = 25 microns) were obtained in the system under optimal conditions, using a small NA focusing lens. However, making a hologram with such a resolution beyond that of human eyes is not sensible. For an authentic hologram, the suggested resolution of the dots is 200 dpi $\sim$ 300 dpi, which suffices to construct a high quality hologram with multiplex images.

Optical interference usually requires an optical bench to isolate the vibrations to make a traditional hologram. However, this isolation is not necessary in this setup because the exposure time of each dot is only tens of milliseconds. Moreover, the asymmetric

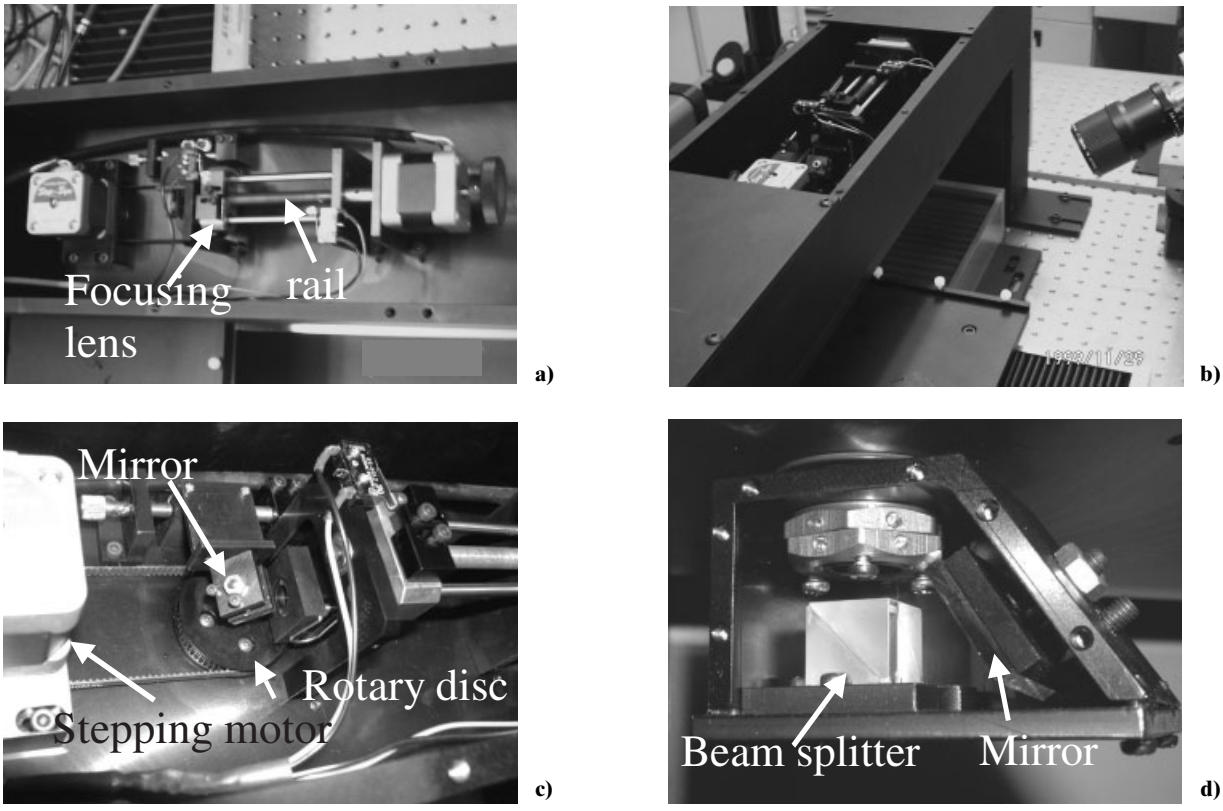

Fig. 8. The pictures of the apparatus for fabricating multiplex image hologram. a) The laser beam splitter, rotary disc and beam spot tuning mechanism. b) The setup of experiment. c) is the photograph of rotary disc that can be driven by the stepping motor to rotate the beam splitting module in d) to change the interference orientation dot by dot.

optical configuration is much simpler than that of the systems considered in references [9–14], that can eliminate the relative vibrations between components. This fact represents an important advantage of not needing to support the entire apparatus on an optical bench. The positive photoresist is used as recording material in the experiment. Shipley AZ-1350 or 1400 are better choices for simpler process. The high contrast developer Shipley #319 is suggested for developing after exposure. An air-cooling He-Cd laser with a wavelength of 442 nm was employed as a light source of the experiment. It supports a shorter exposure time by a factor of around 1/10 the 488 nm or 514 nm output from an argon laser. The stepping resolution of the XY stage is critical for high-resolution recording. The stepping accuracy should be within 1 micron for each moving step. The rotational resolution of the rotational stage is not as critical as that of the XY stage, because a rotational deviation of many seconds will not affect the quality of the images. A clean operation workshop is required to prevent dust from falling on the surface of the photoresist during fabrication. Figure 8 shows photographs of the setup.

4. Coherence and effect grating area issues concerning the asymmetric interference optical setup

The following calculations evaluate problems of the coherent length and the deviation in the shape of the beam spots in the asymmetric setup. According to fig. 9, the optical path difference (OPD) can be expressed as

$$OPD = L_{\text{in}} + P - L_S = L_S(\sec\theta + \tan\theta) - L_S\,, \tag{6}$$

where L_{in} is the optical path length of the incline beam; P is the distance from the beam splitter to the mirror, and L_S is the optical path length of the beam that passes through the beam splitter. The L_S of our system is 40 mm, and the interference angle θ is 21.6 degrees. The OPD is found to be only 18.8 mm. The coherence of a common He-Cd laser exceeds

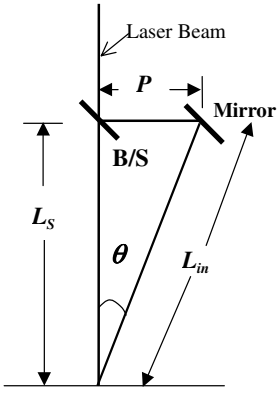

Fig. 9. The schematic diagram of asymmetrical setup of the beam paths in an asymmetric interference setup.

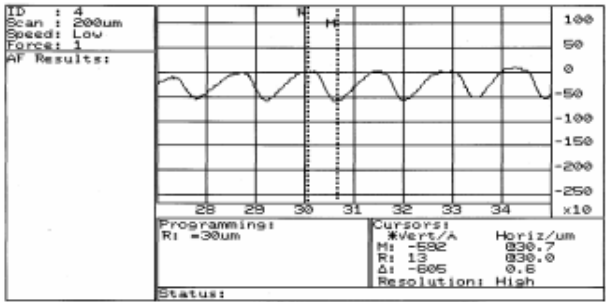

Fig. 10. The surface profile of grating dot detected by Detak 3030ST surface profile meter. The grating period is 1.2 μm interfered from two He-Cd laser beams @442 nm with intersected angle of 21.6 degrees.

300 mm and is sufficiently long to overcome such an OPD distortion. Figure 10 depicts the surface profile of the grating made with the setup discussed here, and measured using by a Dektak 3030ST, with a depth of 60 nm and a period of 1.2 μm. In the experiment, bright images can be reconstructed from the grating fabricated under these conditions. The asymmetry of the beam paths does not reduce their correlation or diffraction efficiency.

The effective area of grating is defined as the overlap ratio of the two beams on the recording plane. According to fig. 11, the effective grating area equals the area of the beam spot at normal incidence, which is smaller than that of an inclined beam. The gray area represents an absence of gratings. Therefore, we can define R_{GA} as the effective grating factor, which is equal to the ratio of area of spot from beam splitter to the area of spot from Mirror:

$$R_{GA} = \frac{(D/2)^2\,\pi}{(D/2)\,(D/2\cos\theta)\,\pi}\,.$$

At $\theta = 21.6$ degrees, R_{GA} is approximately 0.93. Therefore, over 93% illumination efficiency is used to dis-

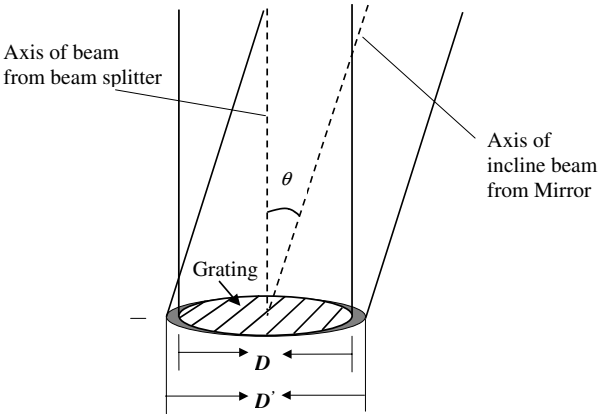

Fig. 11. The overlap of the beam spots from beam splitter and mirror. The gray area has no grating.

play the images. So the mismatch of beam spots due to the asymmetric configuration also does not critically influence the performance of the dot matrix hologram.

5. Discussion

Figure 12a) and b) show microscope photographs of grating dots on the hologram. The diameter of the spot is 100 μm. More images could be interlaced into the hologram using a smaller beam spot. The exposure rate is $10 \sim 15$ dots/sec. The compact configuration can yield tens of exposures by replacing the mechanical shutter with an E-O or A-O shutter, to increase the switching rate. The XY stage is required to respond rapidly to the message from the computer, and to settle quickly after each movement. The setup can be operated without an optical bench, as mentioned in the previous section. Table 1 lists the experimental parameters.

Figures 13 and 14 show samples used in the experiment. Figures 13a) and b) present a portrait of a girl, and a fractal pattern when observed from the left to the right side, obtained from a two-image multiplex hologram. Figures 14a), b), c) and d) show images that displayed from a four-image multiplex anti-counterfeiting hologram on an important document of Taiwan. More images can be interlaced inside a hologram if the

Table 1. The experiment parameters for making a four-images multiplex hologram.

Items	Parameters
He–Cd laser output power	10 mW@442 nm
Interference power intensity	~200 mJ/cm^2
Intersection angle of two laser beams	21.6 degrees
Photoresisit	Shipley AZ1400-30 serious
Developer	MF 319
Exposure time/per dot	$80 \sim 100$ msec
Range of Grating orientation	90 degree (for 4 images)

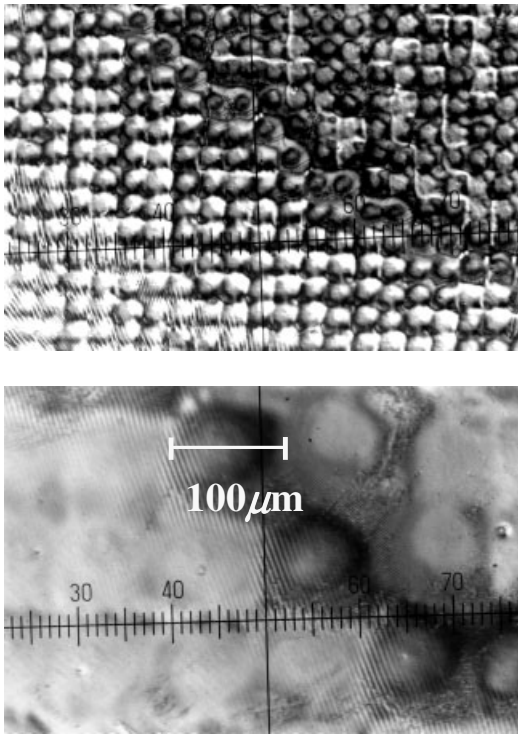

a)

b)

Fig. 12. The microscopic photographs of grating dot hologram. a) The grating dot with diameter of about 100 μm. b) The enlarged photograph of grating dots in the hologram.

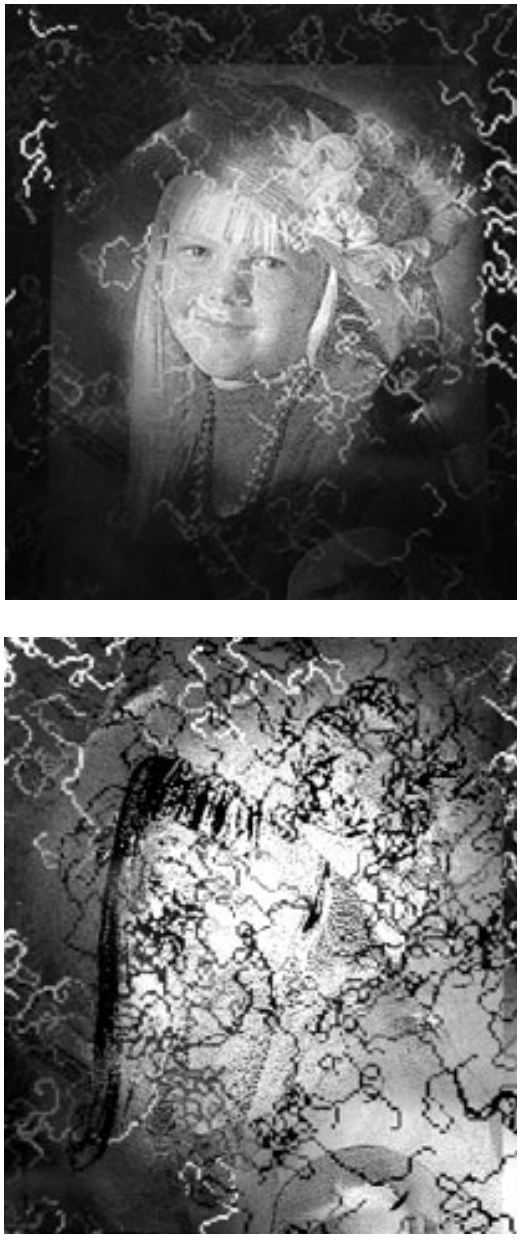

a)

b)

Fig. 13. The images from a multiplex hologram; a) A portrait of a girl appeared while viewing from the left side. b) A fractal pattern appeared while viewing from right side.

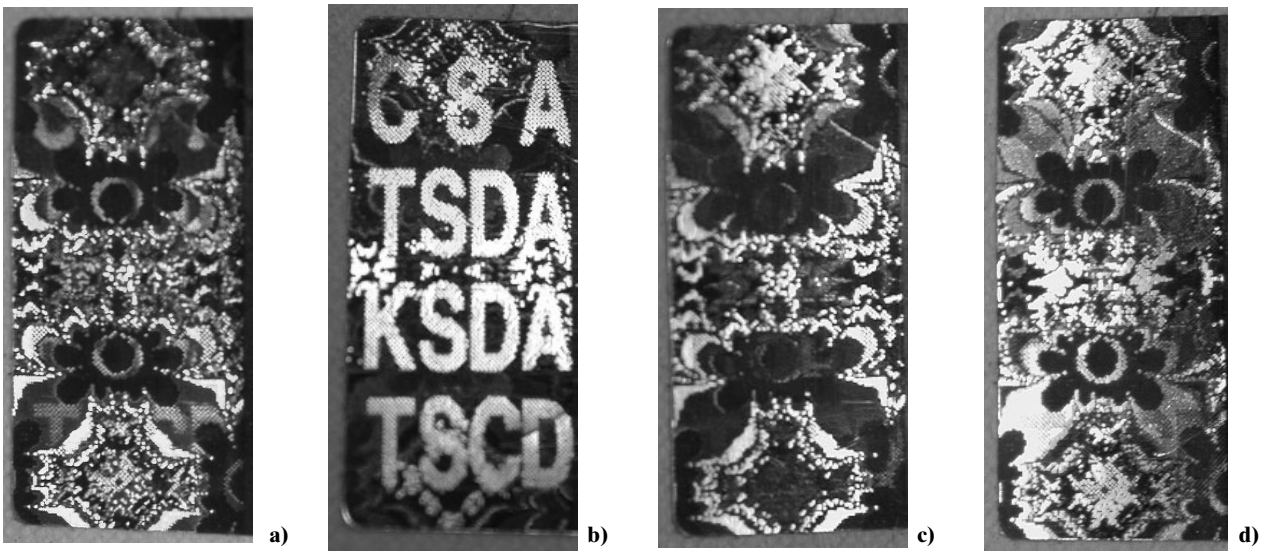

Fig. 14. The images projected from a four images multiplex hologram as a), b), c), d) in different viewing angles, respectively.

size of the grating dots is reduced. However, more time is required for fabrication. The size of grating dot depends upon the size of the hologram and the number of multiplexed images required for a particular security application.

6. Conclusion

The compact configuration with asymmetrical optical setup can effectively support the making of a dot-matrix multiplex hologram as a symmetric setup. Using the fewest optical components, this configuration represents a stable and quick way to make cost-effectively complex security holograms. For advanced authentication applications, the system can fabricate a confidential grating code pattern on a security tag. The tag can be illuminated with a laser beam and detected with a sensor.

Acknowledgments. The authors gratefully acknowledge Miss P. P. Huang, Mr. W. D. Tien and Dr. H. Y. Lin for their support of the project.

References

[1] Leith EN, Upatnieks J: Wavefront reconstruction with diffused illumination and three-dimensional objects. J. Opt. Soc. Am. **54** (1964) 1295–1301
[2] Lesem B, Hirsch PM, Jordan A: Computer synthesis of hologram or 3-D display. Commun. **ACM11** (1968) 661–674
[3] Nakajima M, Mitsuhashi Y: Computer-generated polarization holography: automatic hologram making system and the quality of the reconstructed image. SPIE Proc. **437** (1983) 79–88
[4] Wyrowski F, Hauck R, Bryngdahl O: Computer holography; object dependent deterministic diffusers. Opt. Commun. **63** (1987) 81–84
[5] Benton SA: The reflection alcove hologram; a computer-graphics holographic stereogram. SPIE Proc. **884** (1988) 106–113
[6] Stephen R: Enhanced nondestructive holographic reconstruction. U.S. patent 4,953,924 (1990)
[7] Dorsche RG, Lohman AW, Sinzinger S: Fresnel ping-pong algorithm for two-plane computer-generated holograms display. Appl. Opt. **33** (1994) 864–875
[8] Cai L: Generation of 3D image from computer data with dot array rainbow hologram. SPIE Proc. **2885** (1996) 17–25
[9] Takahashi S: Method for producing a display with a diffraction grating pattern and a display produced by the method. U.S. patent 5,058,992 (October 1991)
[10] Takahashi S, Toda T, Iwada E: Method of manufacturing display having diffraction grating patterns. U.S. patent 5,132,812 (July 1992)
[11] Davis F: Holographic image conversion method for making a controlled holographic grating. U.S. patent 5,262,879 (November 1993)
[12] Newswanger C: Holographic diffraction grating patterns and method for creating the same. U.S. patent 5,291,317 (March 1994)
[13] Davis F: System for making a hologram of an image by manipulating object beam characteristics to reflect image data. U.S. patent 5,822,092 (October 1998)
[14] Yeh SI, Lan JT, Lin HH: Dot matrix hologram for hiding a Moire pattern. U.S. patent 6,317,226 (2001)
[15] Lu YT, Huang BP: The dot matrix hologram fabrication apparatus. U.S. patent 6,043,913 (March 2000)
[16] Goodman JW: Holography, pp. 330–340. McGraw-Hill International Editions, New York 1996
[17] Wilson J, Hawkes J: Modulation of light, pp. 114–115. Prentice Hall, New York 1998
[18] Collier RJ, Burckhardt CB, Lin LH: Optical Holography, pp. 234–240. Academic Press Inc., Boston 1977
[19] Harvey JE, Vernold CL: Description of diffraction grating behavior in direction cosine space. Optics and Photonics News **9** (No. 11) (1998)
[20] Smith HM: Principles of Holography: General theory of volume hologram, pp. 57–68. John Wiley & Sons, New York 1975